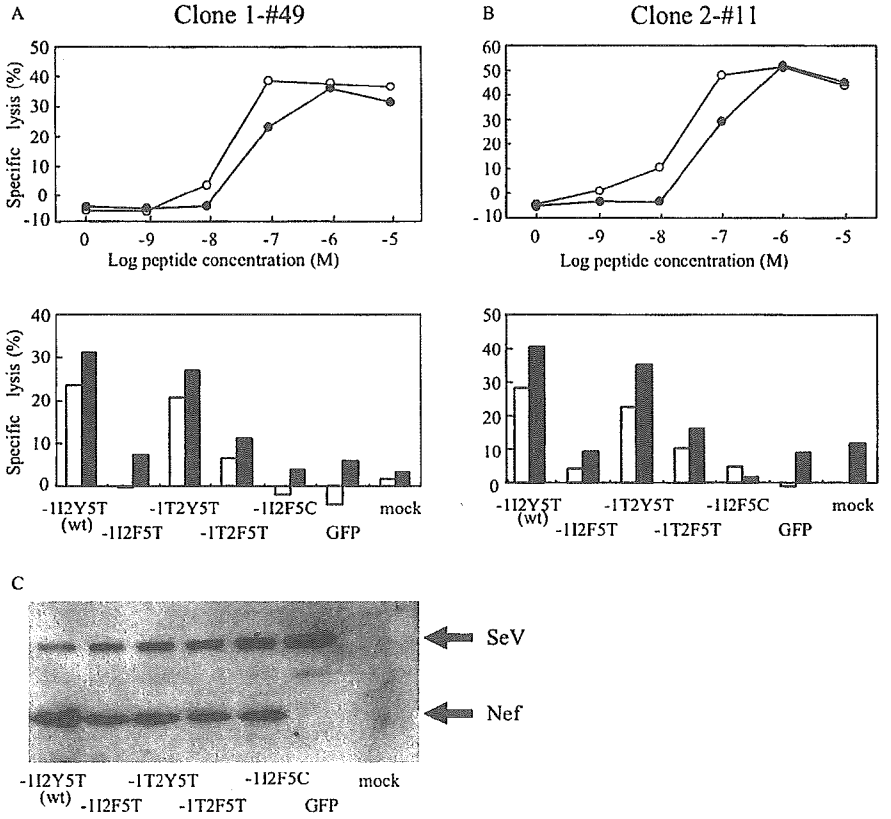

FIG. 5. Killing activity of clone 1-#49 (A) against KWN-T4 target cells pulsed with log-fold dilutions of peptide (top) and expressing native Nef proteins containing wild-type sequences (−1I2Y5T), a Y-to-F substitution at the second position of the CTL epitope (−1I2F5T), an I-to-T substitution at the −1 flanking position (−1T2Y5T), double substitutions at the −1 and second positions (−1T2F5T), and double substitutions at the second and fifth positions (−1I2F5C) (bottom). The effector-versus-target ratio was 1:1 (□) or 2.5:1 (■) in panel A and 1:1 (□) or 4:1 (■) in panel B. Killing activity against KWN-T4 cells infected with control vector expressing green fluorescent protein (GFP) and mock infected (mock) are also shown. (C) Western blot analysis of intracellular expression of various Nef mutants in KWN-T4 target cells. KWN-T4 target cells expressing native Nef proteins containing wild-type sequences (−1I2Y5T), a Y-to-F substitution at the second position of the CTL epitope (−1I2F5T), an I-to-T substitution at the −1 flanking position (−1T2Y5T), double substitutions at the −1 and second positions (−1T2F5T), and double substitutions at the second and fifth positions (−1I2F5C) were examined. KWN-T4 cell lysates infected with control vector expressing GFP and mock infected are also shown. An aliquot (3 μg) of the same KNW-T4 target cells used for the killer assay in the upper panel was used for the Western blot. Symbols: ○, Nef138-10; ●, Nef138-10(2F).

prediction program, NetChop (23), suggested the possibility that the Y-to-F substitution in the second position creates a new cleavage site at the fifth T residue in the CTL epitope. Proteolytic cleavage within the epitope could be the cause of poor antigen presentation.

Although we could not show the process of positive selection for Nef138-10(2F), Nef138-10(2F5C), and Nef138-10(5C), the high prevalence of Nef138-10(2F) in A24-positive patients and the reversion in A24-negative patients suggested that one point mutant, Nef138-10(2F), was selected first, and then two or three point mutants, Nef138-10(2F5C), evolved. Once the T-to-C amino acid substitution at the fifth position is acquired, the binding capacity of the CTL epitope to the HLA-A*2402 heavy chain is abolished (Fig. 3), and the Y-to-F substitution at the second position may become dispensable even in the presence of HLA-A*2402.

In our cohort of patients, Nef138-10(2F) accompanied a −1T substitution in the flanking region very frequently. We observed sequential reversion in the CTL epitope and flanking region at least in one patient with an A24-negative background. As of 11 October 2003, the HIV-1 sequence database showed that the 2F substitution (74 sequences) accompanied the −1T substitution frequently (64.9%) but accompanied the wild-type residue (I) only rarely (9.5%). On the other hand, the wild-type residue (Y) in the second position of the CTL epitope (195 sequences) accompanied wild-type (I) residue more frequently (57.4%) than the −1T substitution (20.5%). Although the function of the region surrounding Nef138-10 has not been elucidated, there seems to be a compensation between these two residues.

In simian immunodeficiency virus infection, CTLs with high functional avidity select for escape variants (29). However, we found CTLs with high functional avidity not only against the wild type but also against Nef138-10(2F) in five patients studied. It is not known how these CTLs against Nef138-10(2F) are maintained in vivo. Very recently, new insights into the exogenous pathway for antigen presentation to CTLs have been elucidated (15, 17). Cross presentation by professional antigen-

presenting cells such as dendritic cells may be responsible. Our study underlines the difficulties in evaluating the effective CTL responses in vivo by CTL assays in which peptides are used, such as ELISPOT.

For example, a CTL escape variant of Epstein-Barr virus was demonstrated in a highly A11-positive population in New Guinea (9). HLA-restricted CTL responses appear to be driving HIV-1 evolution at a population level (20). As far as we know, this is the first direct demonstration of horizontal transmission of CTL escape mutants of HIV-1 at a population level. We previously reported stereotypic amino acid substitutions in HIV-1 at some CTL epitopes restricted by HLA-B35 (21). Stereotypically selected HIV-1 may become dominant through transmission where certain HLA types are highly prevalent. Recently, a rare HLA supertype was shown to have a selective advantage for the prognosis of HIV-1 infection (34). In a population with less diverse HLA types, such as that of Japan, HLA types may have a large impact on HIV-1 evolution and escape. Our study may prove to have important implications for understanding viral pathogenesis and vaccine development.

ACKNOWLEDGMENTS

This work was partly supported by grants for AIDS research from the Ministry of Health, Labor, and Welfare of Japan, a grant-in-aid for Scientific Research (A) from the Japan Society of the Promotion of Science, and the Japan Health Sciences Foundation.

REFERENCES

1. **Anonymous.** 2003. HIV/AIDS in Japan, 2002. Infect. Agents Surveill. Rep. **24:**203–204.
2. **Appay, V., P. R. Dunbar, M. Callan, P. Klenerman, G. M. A. Gillespie, L. Papagno, G. S. Ogg, A. King, F. Lechner, C. A. Spina, S. Little, D. V. Havlir, D. D. Richman, N. Gruener, G. Pape, A. Waters, P. Easterbrook, M. Salio, V. Cerundolo, A. J. McMichael, and S. L. Rowland-Jones.** 2002. Memory CD8$^+$ T cells vary in differentiation phenotype in different persistent virus infections. Nat. Med. **8:**379–385.
3. **Beekman, N. J., P. A. van Veelen, T. van Hall, A. Neisig, A. Sijts, M. Camps, P. M. Kloetzel, J. J. Neefjes, C. J. Melief, and F. Ossendorp.** 2000. Abrogation of CTL epitope processing by single amino acid substitution flanking the C-terminal proteasome cleavage site. J. Immunol. **164:**1898–1905.
4. **Borrow, P., H. Lewicki, B. H. Hahn, G. M. Shaw, and M. B. Oldstone.** 1994. Virus-specific CD8$^+$ cytotoxic T-lymphocyte activity associated with control of viremia in primary human immunodeficiency virus type 1 infection. J. Virol. **68:**6103–6110.
5. **Borrow, P., H. Lewicki, X. Wei, M. S. Horwitz, N. Peffer, H. Meyers, J. A. Nelson, J. E. Gairin, B. H. Hahn, M. B. Oldstone, and G. M. Shaw.** 1997. Antiviral pressure exerted by HIV-1-specific cytotoxic T lymphocytes (CTLs) during primary infection demonstrated by rapid selection of CTL escape virus. Nat. Med. **3:**205–211.
6. **Champagne, P., G. S. Ogg, A. S. King, C. Knabenhans, K. Ellefsen, M. Nobile, V. Appay, G. P. Rizzardi, S. Fleury, M. Lipp, R. Forster, S. Rowland-Jones, R. P. Sekaly, A. J. McMichael, and G. Pantaleo.** 2001. Skewed maturation of memory HIV-specific CD8 T lymphocytes. Nature **410:**106–111.
7. **Collins, K. L., B. K. Chen, S. A. Kalams, B. D. Walker, and D. Baltimore.** 1998. HIV-1 Nef protein protects infected primary cells against killing by cytotoxic T lymphocytes. Nature **391:**397–401.
8. **Couillin, I., B. Culmann-Penciolelli, E. Gomard, J. Choppin, J. P. Levy, J. G. Guillet, and S. Saragosti.** 1994. Impaired cytotoxic T lymphocyte recognition due to genetic variations in the main immunogenic region of the human immunodeficiency virus 1 NEF protein. J. Exp. Med. **180:**1129–1134.
9. **de Campos-Lima, P. O., R. Gavioli, Q. J. Zhang, L. E. Wallace, R. Dolcetti, M. Rowe, A. B. Rickinson, and M. G. Masucci.** 1993. HLA-A11 epitope loss isolates of Epstein-Barr virus from a highly A11+ population. Science **260:**98–100.
10. **Douek, D. C., M. R. Betts, J. M. Brenchley, B. J. Hill, D. R. Ambrozak, K. L. Ngai, N. J. Karandikar, J. P. Casazza, and R. A. Koup.** 2002. A novel approach to the analysis of specificity, clonality, and frequency of HIV-specific T cell responses reveals a potential mechanism for control of viral escape. J. Immunol. **168:**3099–3104.
11. **Foung, S. K., B. Taidi, D. Ness, and F. C. Grumet.** 1986. A monoclonal antibody against HLA-A11 and A24. Hum. Immunol. **15:**316–319.
12. **Goulder, P. J., C. Brander, Y. Tang, C. Tremblay, R. A. Colbert, M. M. Addo, E. S. Rosenberg, T. Nguyen, R. Allen, A. Trocha, M. Altfeld, S. He, M. Bunce, R. Funkhouser, S. I. Pelton, S. K. Burchett, K. McIntosh, B. T. Korber, and B. D. Walker.** 2001. Evolution and transmission of stable CTL escape mutations in HIV infection. Nature **412:**334–338.
13. **Goulder, P. J., A. Edwards, R. E. Phillips, and A. J. McMichael.** 1997. Identification of a novel HLA-A24-restricted cytotoxic T-lymphocyte epitope within HIV-1 Nef. AIDS **11:**1883–1884.
14. **Goulder, P. J., R. E. Phillips, R. A. Colbert, S. McAdam, G. Ogg, M. A. Nowak, P. Giangrande, G. Luzzi, B. Morgan, A. Edwards, A. J. McMichael, and S. Rowland-Jones.** 1997. Late escape from an immunodominant cytotoxic T-lymphocyte response associated with progression to AIDS. Nat. Med. **3:**212–217.
15. **Guermonprez, P., L. Saveanu, M. Kleijmeer, J. Davoust, P. Van Endert, and S. Amigorena.** 2003. ER-phagosome fusion defines an MHC class I cross-presentation compartment in dendritic cells. Nature **425:**397–402.
16. **Ho, S. N., H. D. Hunt, R. M. Horton, J. K. Pullen, and L. R. Pease.** 1989. Site-directed mutagenesis by overlap extension using the polymerase chain reaction. Gene **77:**51–59.
17. **Houde, M., S. Bertholet, E. Gagnon, S. Brunet, G. Goyette, A. Laplante, M. F. Princiotta, P. Thibault, D. Sacks, and M. Desjardins.** 2003. Phagosomes are competent organelles for antigen cross-presentation. Nature **425:**402–406.
18. **Ikeda-Moore, Y., H. Tomiyama, K. Miwa, S. Oka, A. Iwamoto, Y. Kaneko, and M. Takiguchi.** 1997. Identification and characterization of multiple HLA-A24-restricted HIV-1 CTL epitopes: strong epitopes are derived from V regions of HIV-1. J. Immunol. **159:**6242–6252.
19. **Imanishi, T., T. Akaza, A. Kimura, K. Tokunaga, and T. Gojobori.** 1992. Allele and haplotype frequencies for HLA and complement loci in various ethnic groups, p. 1065–1220. *In* K. Tsuji, M. Aizawa, and T. Sasazuki (ed.), HLA 1991, vol. 1. Oxford University Press.
20. **Jost, S., M. C. Bernard, L. Kaiser, S. Yerly, B. Hirschel, A. Samri, B. Autran, L. E. Goh, and L. Perrin.** 2002. A patient with HIV-1 superinfection. N. Engl. J. Med. **347:**731–736.
21. **Kawana, A., H. Tomiyama, M. Takiguchi, T. Shioda, T. Nakamura, and A. Iwamoto.** 1999. Accumulation of specific amino acid substitutions in HLA-B35-restricted human immunodeficiency virus type 1 cytotoxic T lymphocyte epitopes. AIDS Res. Hum. Retrovir. **15:**1099–1107.
22. **Kawana-Tachikawa, A., M. Tomizawa, J. Nunoya, T. Shioda, A. Kato, E. E. Nakayama, T. Nakamura, Y. Nagai, and A. Iwamoto.** 2002. An efficient and versatile mammalian viral vector system for major histocompatibility complex class I/peptide complexes. J. Virol. **76:**11982–11988.
23. **Kesmir, C., A. K. Nussbaum, H. Schild, V. Detours, and S. Brunak.** 2002. Prediction of proteasome cleavage motifs by neural networks. Protein Eng. **15:**287–296.
24. **Koup, R. A., J. T. Safrit, Y. Cao, C. A. Andrews, G. McLeod, W. Borkowsky, C. Farthing, and D. D. Ho.** 1994. Temporal association of cellular immune responses with the initial control of viremia in primary human immunodeficiency virus type 1 syndrome. J. Virol. **68:**4650–4655.
25. **Kuzushima, K., N. Hayashi, H. Kimura, and T. Tsurumi.** 2001. Efficient identification of HLA-A*2402-restricted cytomegalovirus-specific CD8(+) T-cell epitopes by a computer algorithm and an enzyme-linked immunospot assay. Blood **98:**1872–1881.
26. **McMichael, A. J., and R. E. Phillips.** 1997. Escape of human immunodeficiency virus from immune control. Annu. Rev. Immunol. **15:**271–296.
27. **Migueles, S. A., A. C. Laborico, W. L. Shupert, M. S. Sabbaghian, R. Rabin, C. W. Hallahan, D. Van Baarle, S. Kostense, F. Miedema, M. McLaughlin, L. Ehler, J. Metcalf, S. Liu, and M. Connors.** 2002. HIV-specific CD8$^+$ T cell proliferation is coupled to perforin expression and is maintained in nonprogressors. Nat. Immunol. **3:**1061–1068.
28. **Moore, C. B., M. John, I. R. James, F. T. Christiansen, C. S. Witt, and S. A. Mallal.** 2002. Evidence of HIV-1 adaptation to HLA-restricted immune responses at a population level. Science **296:**1439–1443.
29. **O'Connor, D. H., T. M. Allen, T. U. Vogel, P. Jing, I. P. DeSouza, E. Dodds, E. J. Dunphy, C. Melsaether, B. Mothe, H. Yamamoto, H. Horton, N. Wilson, A. L. Hughes, and D. I. Watkins.** 2002. Acute phase cytotoxic T lymphocyte escape is a hallmark of simian immunodeficiency virus infection. Nat. Med. **8:**493–499.
30. **Ogg, G. S., X. Jin, S. Bonhoeffer, P. R. Dunbar, M. A. Nowak, S. Monard, J. P. Segal, Y. Cao, S. L. Rowland-Jones, V. Cerundolo, A. Hurley, M. Markowitz, D. D. Ho, D. F. Nixon, and A. J. McMichael.** 1998. Quantitation of HIV-1-specific cytotoxic T lymphocytes and plasma load of viral RNA. Science **279:**2103–2106.
31. **Phillips, R. E., S. Rowland-Jones, D. F. Nixon, F. M. Gotch, J. P. Edwards, A. O. Ogunlesi, J. G. Elvin, J. A. Rothbard, C. R. Bangham, C. R. Rizza, et al.** 1991. Human immunodeficiency virus genetic variation that can escape cytotoxic T cell recognition. Nature **354:**453–459.
32. **Schwartz, O., V. Marechal, S. Le Gall, F. Lemonnier, and J. M. Heard.** 1996. Endocytosis of major histocompatibility complex class I molecules is induced by the HIV-1 Nef protein. Nat. Med. **2:**338–342.
33. **Tomiyama, H., H. Akari, A. Adachi, and M. Takiguchi.** 2002. Different effects of Nef-mediated HLA class I down-regulation on human immunode-

ficiency virus type 1-specific CD8+ T-cell cytolytic activity and cytokine production. J. Virol. 76:7535–7543.
34. **Trachtenberg, E., B. Korber, C. Sollars, T. B. Kepler, P. T. Hraber, E. Hayes, R. Funkhouser, M. Fugate, J. Theiler, Y. S. Hsu, K. Kunstman, S. Wu, J. Phair, H. Erlich, and S. Wolinsky.** 2003. Advantage of rare HLA supertype in HIV disease progression. Nat. Med. 9:928–935.
35. **Watanabe, N., M. Tomizawa, A. Tachikawa-Kawana, M. Goto, A. Ajisawa, T. Nakamura, and A. Iwamoto.** 2001. Quantitative and qualitative abnormalities in HIV-1-specific T cells. AIDS 15:711–715.
36. **Yamada, T., N. Kaji, T. Odawara, J. Chiba, A. Iwamoto, and Y. Kitamura.** 2003. Proline 78 is crucial for human immunodeficiency virus type 1 Nef to down-regulate class I human leukocyte antigen. J. Virol. 77:1589–1594.

Influence of single-nucleotide polymorphisms in the multidrug resistance-1 gene on the cellular export of nelfinavir and its clinical implication for highly active antiretroviral therapy

*Dayong Zhu[1], Hitomi Taguchi-Nakamura[1], Mieko Goto[1], Takashi Odawara[2], Tetsuya Nakamura[2], Harumi Yamada[3], Hajime Kotaki[3], Wataru Sugiura[4], Aikichi Iwamoto[1,2] and Yoshihiro Kitamura[1]**

[1]Division of Infectious Diseases, Advanced Clinical Research Centre, Institute of Medical Science, University of Tokyo, Tokyo, Japan
[2]Department of Infectious Diseases and Applied Immunology, Institute of Medical Science, University of Tokyo, Tokyo, Japan
[3]Department of Pharmacy, Research Hospital, Institute of Medical Science, University of Tokyo, Tokyo, Japan
[4]National Institute of Infectious Diseases, Tokyo, Japan

*Corresponding author: +81 3 5449 5336; Fax: +81 3 5449 5427; E-mail: yochan@ims.u-tokyo.ac.jp

Protease inhibitors (PIs) such as nelfinavir (NFV) suppress HIV replication. PIs are substrates of P-glycoprotein (P-gp), the product of the multidrug-resistance-1 (*MDR1*) gene. Three single-nucleotide polymorphisms (SNPs) are present in exons of the *MDR1* gene: *MDR1* 1236, *MDR1* 2677 and *MDR1* 3435. We speculated that these genetic polymorphisms affected PI concentration in the cell. To verify this hypothesis, we first genotyped these SNPs in 79 Japanese patients by the SNaPshot method and found incomplete linkage disequilibrium between the SNPs. Because the SNP at *MDR1* 3435 has been reported to be associated with P-gp expression, we evaluated the effect of that SNP on the export of NFV from HIV-positive patients' lymphoblastoid cell lines by measuring time-dependent decrease in the amount of intracellular NFV by high-performance liquid chromatography. We found the intracellular concentration of NFV in lymphoblastoid cell lines (LCLs) with the homozygous T/T genotype at *MDR1* 3435 were higher than that with C/C genotype with statistical significance. This suggests that the activity of P-gp in patients' LCL cells with the *MDR1* 3435 T/T genotype was lower. In a retrospective study we evaluated the effect of the SNPs on CD4 cell count recovery in response to antiretroviral treatment with PIs, and obtained statistically significant evidence that suggested marginal association of the SNP at *MDR1* 1236 but not at *MDR1* 2677 or *MDR1* 3435. As *in vitro* results were not consistent with the clinical evaluation, clinical importance of *MDR1* genotyping for antiretroviral therapy remains to be investigated in a larger, case-controlled study.

Introduction

Antiretroviral therapy with HIV protease inhibitors (PIs) in combination with reverse transcriptase inhibitors dramatically improved the prognosis of patients infected with HIV-1. However, some patients fail to achieve the maximal virological suppression. We speculate that such failure is partly because PIs do not accumulate in lymphocytes in their active free forms in a concentration high enough to inhibit viral replication [1,2], although the intracellular active PI levels have, to the best of our knowledge, not yet been determined. The activity of P-glycoprotein (P-gp), the product of the multidrug resistance-1 (*MDR1*) gene, appears to affect intracellular PI concentration, because PIs such as nelfinavir (NFV) are substrates of P-gp [2]. P-gp is a glycosylated membrane protein belonging to the ATP-binding cassette superfamily of membrane transporters. P-gp is expressed in many tissues and cell types including intestinal epithelial cells and lymphocytes, where it acts as an energy-dependent exporter [3–9]. The *MDR1* is polymorphic and at least three single-nucleotide polymorphisms (SNPs) have been identified in the exons in a healthy Japanese population [10] as well as in other ethnic groups [6]. *MDR1* 1236 and *MDR1* 3435 are silent mutations in exons 12 and 26 [3,11], respectively, whereas *MDR1* 2677 is a substitution mutation in exon 21 [11]. Reportedly, the SNP at *MDR1* 3435 is associated with the amount and activity of P-gp protein both *in vitro* and *in vivo* [3,12]. In addition, individuals with the T/T genotype at *MDR1* 3435 were found to express less P-gp in lymphocytes and in intestinal epithelial cells [3,13] and showed lower efflux of rhodamine from natural killer (NK)

©2004 International Medical Press 1359-6535/02/$17.00

cells than those with the C/C genotype [13]. According to these observations, *MDR1* polymorphisms seem to affect the intracellular PI concentration and the outcome of antiretroviral treatment. However, the role of *MDR1* 3435 SNP in the response to antiretroviral therapy is still controversial [12,14].

The objective of this study was to evaluate the effect of three *MDR1* SNPs on the intracellular concentrations of NF and to evaluate the impact of those SNPs on virological and immunological response to antiretroviral treatment, including NFV and PIs. We genotyped the SNPs in 79 Japanese patients and compared the velocity of NFV efflux among selected patients' lymphoblastoid cell lines (LCLs) with different *MDR1* 3435 genotypes. We also analysed the viral loads and CD4 cell counts after initiation of antiretroviral treatment with prescriptions with PIs including NFV in 21 patients.

Materials and methods

Patients

A total of 79 HIV-positive Japanese patients were enrolled in this study. These patients attended a hospital AIDS clinic at the Institute of Medical Science, University of Tokyo (IMSUT). The patients provided their written informed consent to participate in the study and to supply blood samples for DNA analysis and cell culture. Of the 79 patients, 21 receiving highly active antiretroviral therapy (HAART) including PIs were divided into three groups: 11 patients receiving HAART with NFV, four patients receiving HAART with indinavir (IDV) and six patients receiving HAART with saquinavir (SQV) or lopinavir/ritonavir (LPV/RTV). CD4 cell counts and HIV-RNA of plasma were analysed for 9 months after the initiation of the antiretroviral treatment. The study has been approved by the ethics committee of IMSUT.

Single-nucleotide polymorphisms

We typed three single-nucleotide polymorphisms (SNPs) at *MDR1* 1236 (exon 12), *MDR1* 2677 (exon 21) and *MDR1* 3435 (exon 26) by polymerase chain reaction (PCR) followed by ABI PRISM SNaPshot Multiplex Kit (PE Biosystems, Foster City, Calif., USA) [15]. Information on primers and conditions for PCR was obtained at http://snp.ims.u-tokyo.ac.jp [10].

Cells and determination of uptake and efflux of NFV

Peripheral blood mononuclear cells (PBMCs) were separated from patients' whole blood with Ficoll-Conray gradient centrifugation. LCLs were obtained by transforming PBMCs with Epstein-Barr virus (EBV), which was obtained from cell-free supernatants of EBV-producing B95-8 cell lines [16]. LCLs were maintained in RPMI 1640 medium (Sigma-Aldrich, St. Louis, Mo., USA) supplemented with 10% heat-inactivated fetal calf serum.

{Author: OK?}

To determine the time course of NFV uptake into LCL cells, LCL cells (1×10^6/10 ml, counted with a haematocytometer) were incubated at 37°C in a medium containing 10 μM NFV. Cells were harvested by centrifugation at 1500 ×*g* for 5 min at 4°C and immediately frozen at −80°C until high-performance liquid chromatography (HPLC) analysis. To determine the velocity of NFV efflux from LCL cells, these patients' LCL cells were incubated at 37°C in a medium containing 10 μM NFV for 3 h. The cells were then quickly washed twice with 10 ml ice-cold phosphate-buffered saline and cultured in 10 ml NFV-free medium for up to 3 h. After an interval, aliquot cells were harvested by centrifugation at 1500 ×*g* for 5 min at 4°C and immediately frozen at −80°C until HPLC analysis.

Reverse transcription-PCR (RT-PCR)

For quantification of *MDR1* transcript, RNA from 1×10^7 LCL cells was isolated using Trizol reagents (Invitrogen Corp, Carlsbad, Calif., USA). First strand cDNA was obtained by using ReverTra Ace (Toyobo, Osaka, Japan) with 1 μg of total RNA. cDNA was subjected to PCR. Information on primers and conditions for PCR was obtained as previously described [17]. We used human glyceraldehyde 3-phosphate dehydrogenase mRNA as a positive control.

Determination of intracellular concentration of NFV by HPLC

The patients' frozen LCL cells were extracted with 1.5 ml of ethanol. The extracts were then clarified by centrifugation at 2050 ×*g* for 10 min at 4°C. The ethanol extracts were evaporated at 30°C and dissolved in 180 μl of mobile phase, which was a mixture of phosphate buffer (containing 50 mM KH_2PO_4 and 50 mM Na_2HPO_4; pH 5.63) and acetonitrile (1:1, v:v) [18]. The amounts of NFV were measured using a Sensyu Pack ODS C_{18} column (5 μm particle size; 150×4.6 mm, Sensyu Scientific Co, Tokyo, Japan) at a flow rate of 1.5 ml/min by HPLC (Shimadzu Co, Tokyo, Japan). The UV detection wave length was 220 nm and efavirenz (EFV) was used as an internal standard. The lower limits of detection and quantification were 20 ng (30.1 pmole)/10^6 cells, and the calibration range was 20–2000 ng (30.1–3010 pmole/10^6 cells).

Results

We typed the three SNPs at *MDR1* 1236 (exon 12), *MDR1* 2677 (exon 21) and *MDR1* 3435 (exon 26) in DNA samples from 79 HIV-positive Japanese patients

©2004 International Medical Press

(Figure 1). We found that it was consistent with the Hardy–Weinberg principle (Tables 1 and 2). Furthermore, in all possible two-way comparisons of the three SNPs at *MDR1* 1236 (exon 12), *MDR1* 2677 (exon 21, excluding the genotypes containing G) and *MDR1* 3435 (exon 26), we found significant linkage disequilibrium between *MDR1* 2677 A (T) and *MDR1* 1236 C (T), *MDR1* 2677 A (T) and *MDR1* 3435 C (T), and *MDR1* 1236 C (T) and *MDR1* 3435 C (T), respectively.

Figure 1. Frequency of SNPs in *MDR1*

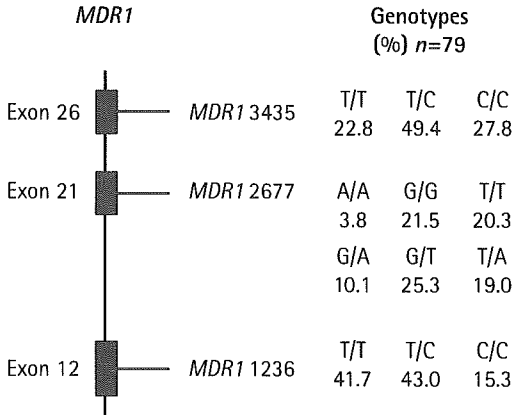

The SNPs at *MDR1* 1236, *MDR1* 2677 and *MDR1* 3435 were typed by the SNaPshot method. Genotype frequencies at each site are shown as percentage among 79 HIV-infected Japanese patients. The thin vertical line at left represents the *MDR1* gene on human chromosome 7. The closed boxes represent exons 12, 21 and 26.

Table 1. Hardy–Weinberg principle at *MDR1* 1236 (*n*=79)

	T/T	T/C	C/C
Observed number of patients	33	34	12
Expected number of patients	31.7*	36.7†	10.6‡

p: Frequency for the T allele $\frac{33\times2+34}{2\times79}=0.633$

q: Frequency for the C allele 1−p=0.367

*$79\times p^2=31.7$

†$79\times2pq=36.7$

‡$9\times q^2=10.6$

Table 2. Hardy–Weinberg principle at *MDR1* 3435 (*n*=79)

	T/T	T/C	C/C
Observed number of patients	18	39	22
Expected number of patients	17.8*	39.4†	21.8‡

p: Frequency for the T allele $\frac{18\times2+39}{2\times79}=0.475$

q: Frequency for the C allele 1−p=0.525

*$79\times p^2=17.8$

†$79\times2pq=39.4$

‡$79\times q^2=21.8$

Reportedly, *MDR1* 3435 T/T genotype was associated with lower expression of P-gp in leukocytes [13] so we hypothesized that the genotype was also associated with slower cellular export of NFV in patients' lymphocytes. To investigate this, we first established LCLs by immobilizing selected patients' PBMCs with EBV. We selected eight patients' LCLs with *MDR1* 3435 C/C (*n*=4) and T/T (*n*=4) and verified similar levels of *MDR1* in these LCLs by RT-PCR (Figure 2). We observed little variation in *MDR1* transcripts.

We found that uptake of NFV was rapid into LCLs reaching a steady-state within 5 mins (Figure 3). We studied four patients' LCLs with *MDR1* 3435 T/T and *MDR1* 3435 C/C to compare the steady-state intracellular concentration of NFV after 3 h incubation in a medium containing 10 μM NFV. The intracellular concentrations of NFV in LCLs with *MDR1* 3435 T/T and C/C genotypes were 2593 μM and 2411 μM, respectively (*n*=4), with no statistical difference. We calculated these values by hypothesizing that the LCLs are ideal spheres (10 μm diameter) and that NFV distributes uniformly in the cell.

We then compared NFV efflux from those LCLs with different genotypes at *MDR1* 3435. Before measuring export of NFV, LCLs were cultured with NFV to a saturated level. These NFV-loaded cells were transferred to NFV-free medium and cultured for 3 h with intermittent sampling of cell aliquots. We compared the efflux of NFV from the eight patients' LCLs with *MDR1* 3435 T/T and C/C (*n*=4 each), which had been verified to express *MDR1* mRNA by

Figure 2. *MDR1* mRNA expression in LCLs

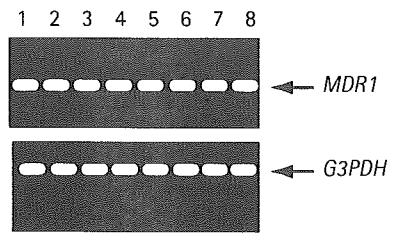

We selected eight patients' LCLs with *MDR1* 3435 C/C (lanes 1–4) and T/T (lanes 5–8) and measured the expression of *MDR1* mRNA. Total cellular RNA from LCLs was subjected to RT-PCR with primer sets for *MDR1* and *G3PDH* transcripts. Aliquots were subjected to agarose gel electrophoresis. The genotypes at *MDR1* 1236, 2677 and 3435: lanes 1 and 2, (T/T, G/G, C/C); lane 3, (T/C, G/A, C/C); lane 4 (C/C G/A C/C); lane 5 (T/T, G/T, T/T); and lanes 6–8 (T/T, T/T, T/T).

{Author: OK?}

RT-PCR (Figure 2). The concentration of intracellular NFV in LCLs with the homozygous T/T genotype at *MDR1* 3435 was higher than in those with C/C genotype at 120 mins and 180 mins. This difference was statistically significant (P=0.04 and 0.02, respectively, Mann–Whitney U-test, Figure 4). This meant the NFV efflux in patients' LCL cells with the *MDR1* 3435 T/T genotype was slower than that with C/C genotype. Thus, we suspect the activity of P-gp in patients' LCLs with the *MDR1* 3435 T/T genotype is lower than that with the C/C genotype.

Figure 3. A typical time course of NFV uptake

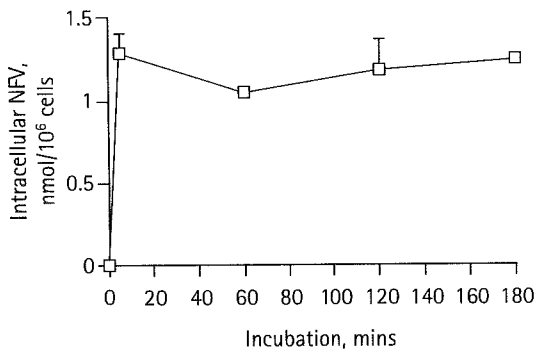

LCL cells (1 ×10⁶/10 ml) were incubated in medium containing 10 μM of NFV. Cells were harvested at 0, 5, 60, 120 and 180 mins and assayed for intracellular NFV by HPLC. The horizontal axis shows the incubation time in mins. The vertical axis shows the intracellular amount of NFV per 10^6 cells. The error bars represent the standard deviations.

Figure 4. NFV efflux from patients' LCLs

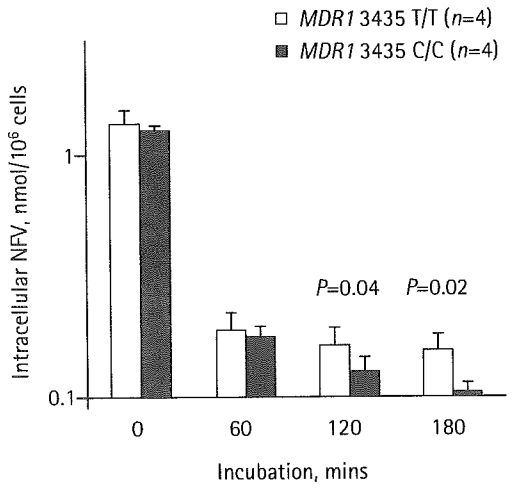

LCL cells were incubated in medium containing 10 μM of NFV for 3 h. Cells were then washed and cultured in NFV-free medium. Intracellular concentration of NFV was determined at 0, 60, 120 and 180 mins by HPLC. The horizontal axis shows the incubation time in mins. The vertical axis shows the intracellular amount of NFV per 10^6 cells. We selected eight patients (described in the legend to Figure 2) and examined the velocity of NFV efflux from those cells. The intracellular concentration of NFV was measured several times in all patients' LCLs, and data were similar in every test. The error bars represent the standard deviations.

To examine the influence of *MDR1* 3435 genotypes on the response to treatment, we assessed increase in CD4 cell counts and viral suppression in 21 patients after initiation of HAART. At first, we hoped to analyse data obtained from a group of patients receiving NFV alone as a PI, but could not, due to the small number of NFV-receiving patients. Thus, we carried out the analysis in those patients receiving PIs including NFV (n=11), indinavir (n=4) and saquinavir/lopinavir/ritonavir (n=6). CD4 cell counts before treatment were similar among patients with various genotypes. Patients with various genotypes at *MDR1* 3435 showed similar changes in CD4 cell counts (Figure 5A) and viral suppression (Figure 6A) during 9 months of HAART. We found patients with the *MDR1* 1236 T/T showed higher increase in CD4 cell counts at 1 month (148 cells/μl) and 9 months (264 cells/μl) after initiation of therapy than those with *MDR1* 1236 C/C (20 cells/μl and 34 cells/μl, respectively) (Figure 5C). We suspected that *MDR1* 1236 T/T was associated with a higher rate of recovery of CD4 cell counts for patients receiving HAART with PI. We did not find differences in rates of viral suppression among the patients with various *MDR1* 1236 genotypes (Figure 6C). We did not observe a statistical difference in CD4 cell counts or viral loads among patients with different *MDR1* 2677 genotypes (Figures 5B and 6B).

Discussion

In this study, we genotyped three SNPs at *MDR1* 1236 (exon 12), *MDR1* 2677 (exon 21) and *MDR1* 3435 (exon 26) (Figure 1) in 79 HIV-positive Japanese patients and found incomplete linkage disequilibrium – as has also been reported in other ethnic groups [6]. We found that genotype frequencies of the SNPs at *MDR1* 1236 (exon 12) and *MDR1* 3435 (exon 26) in this population were in Hardy–Weinberg equilibrium. This suggested that the studied population was precisely genotyped and unbiased in terms of the *MDR1* gene. We compared the activity of P-gp among patients' LCLs with different *MDR1* 3435 genotypes by measuring NFV efflux from the cultured LCL cells by HPLC. We found that the intracellular concentration of NFV in LCLs with the homozygous T/T genotype at *MDR1* 3435 was higher than in those with the C/C genotype at 120 mins and 180 mins. This difference was statistically significant (P=0.04 and 0.02, respectively; Mann–Whitney U-test; Figure 4). In contrast, in the retrospective evaluation of 21 HIV-positive patients

©2004 International Medical Press

Figure 5. Increase in CD4 cell count among patients with the various genotypes of *MDR1* during antiretroviral treatment

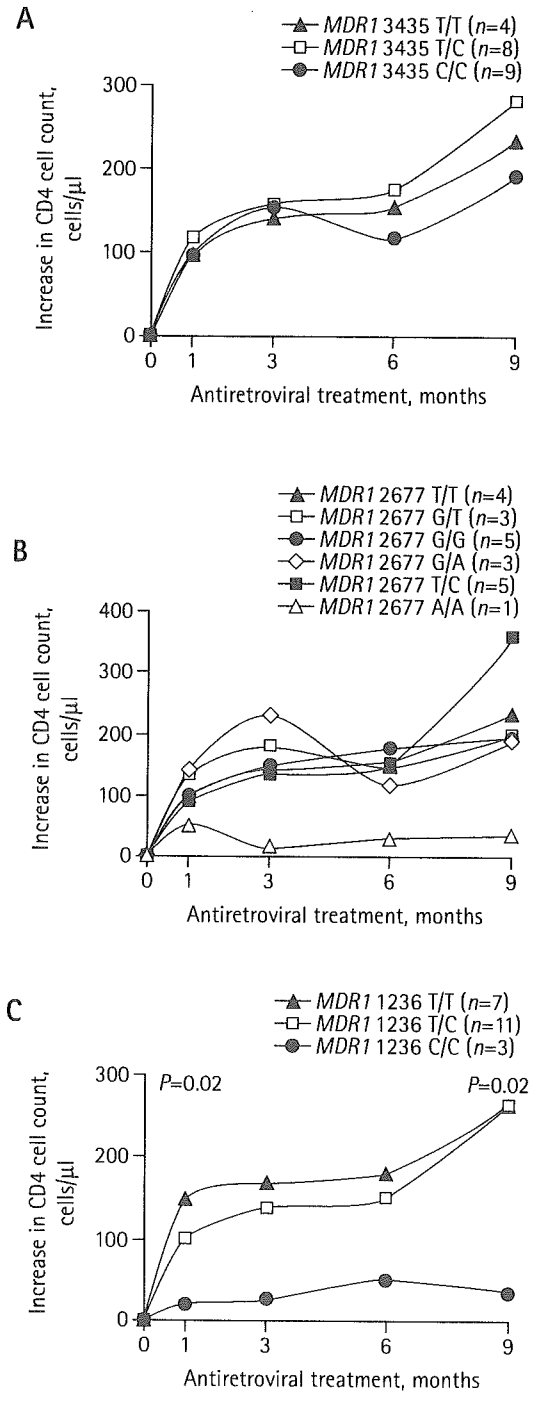

We assessed increase in CD4 cell counts among 21 patients. Every subject had CD4 cell counts and viral loads at months 0, 1, 3, 6 and 9. **(A)** *MDR1* 3435: T/T (▲); C/C (●); T/C (□). **(B)** *MDR1* 2677: T/T (▲); G/G (●); G/T (□); G/A (◇); T/A (■); A/A (△). **(C)** *MDR1* 1236: T/T (▲); C/C (●); T/C (□). The vertical axis shows the increase in CD4 cell count during treatment. *P* values were calculated by the Mann–Whitney U-test.

Figure 6. Suppression of viraemia among patients with various genotypes of MDR1 after antiretroviral treatment

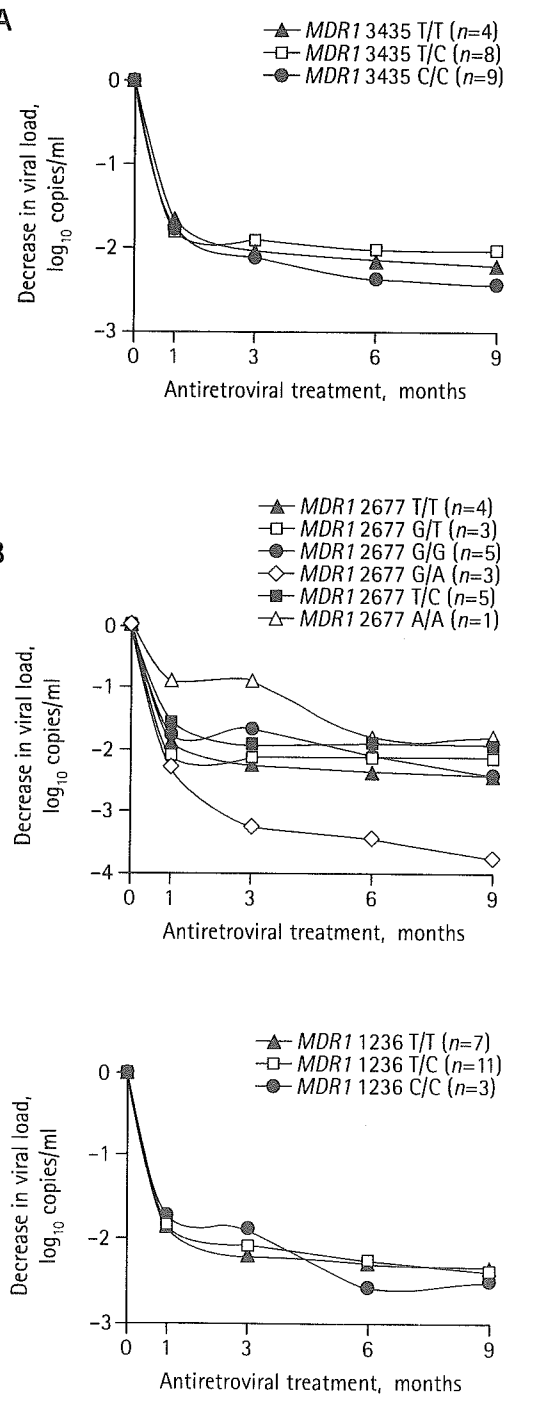

We assessed suppression of viraemia among the same 21 patients as described in the legend to Figure 5. **(A)** *MDR1* 3435: T/T (▲); C/C (●); T/C (□). **(B)** *MDR1* 2677: T/T (▲); G/G (●); G/T (□); G/A (◇); T/A (■); A/A (▲). **(C)** *MDR1* 1236: T/T (▲); C/C (●); T/C (□). The vertical axis shows decrease in viral load. Values are shown as $\log_{10}$ copies/ml plasma.

receiving PIs, we failed to observe a statistical difference in CD4 cell counts and viral suppression among patients with different *MDR1* 3435 SNPs (Figures 5A and 6A). Furthermore, we found that patients with the *MDR1* 1236 T/T genotype showed a greater increase in the CD4 cell counts during HAART therapy with PI at months 1 and 9 than patients with the *MDR1* 1236 C/C genotype (Figure 5C). The contribution of genetic variations in the *MDR1* gene to the patients' clinical characteristics, if any, seems very complicated and thus is difficult to evaluate in a straightforward manner.

As the steady-state intracellular concentration of NFV was about 250 times higher than that in the medium (10 μM), the uptake of NFV seems active rather than passive. However, these *in vitro* data depart from what has been observed in *in vivo* measurements of NFV in patients [19,20] presumably due to the presence of alpha(1)-acid glycoprotein to which NFV binds in plasma [21]. Furthermore, this discrepancy may also be due to the differential distribution of NFV among tissues rather than in free artificial medium. Therefore, our *in vitro* data should be considered as such, that is, *in vivo* lymphocytes may be unlikely to have this high intracellular to extracellular concentration ratio (250:1).

We observed an association of slower efflux of NFV *in vitro* with the T/T genotype at *MDR1* 3435. In fact, P-gp has been found to export PIs from lymphocytes and reduce their anti-HIV activity *in vitro*, and its low activity has been found to be associated with the T/T genotype at *MDR1* 3435 [13]. As the SNP at *MDR1* 3435 is a silent mutation, one possible explanation for this association is that the T/T genotype at *MDR1* 3435 renders *MDR1* mRNA unstable in the cell. Another possible explanation for the association is that *MDR1* 3435 SNP is in linkage disequilibrium with the SNPs at *MDR1* 1236 (exon 12) and *MDR1* 2677 (exon 21), the latter of which is a substitution mutation. This amino acid substitution from the *MDR1* 2677 SNP may be responsible for the observed difference (Figure 4) [11]. Another possible explanation is that *MDR1* 3435 SNPs are in linkage disequilibrium with a polymorphism(s) elsewhere in the genome that modifies *MDR1* expression or function [3,12].

Although an *in vitro* study showed that the velocity of NFV efflux in patients' LCLs with the *MDR1* 3435 T/T genotype was slower than that with the C/C genotype, we failed to observe a statistical difference in CD4 cell counts and viral suppression among patients with different *MDR1* 3435 genotypes (Figures 5A and 6A). Four equally possible accounts seem to explain this discrepancy. Firstly, since the C/C genotype at *MDR1* 3435 is also correlated with higher expression of P-gp in intestinal epithelial cells that adsorb PIs, the *MDR1* 3435 C/C is likely to be associated with higher absorption of PIs and higher PI concentration in plasma [12,22]. The higher plasma levels of NFV in 3435 C/C patients in one study [12] is puzzling and as yet not fully understood. Secondly, the sample size (n=21) in this study may be too small to evaluate CD4 cell counts or viral suppression in a statistical way. Thirdly, since the enrolled patients received different treatment combinations of PIs and reverse transcription inhibitors during antiretroviral therapy, the clinical evaluation was not normalized. Finally, because LCLs – immobilized B cells – but not CD4+ T cells were used in this study, the function of P-gp in a setting of HIV-1 infection may not have been accurately tested. In contrast to the *MDR1* 3435, we observed a marginal but statistically significant association of the *MDR1* 1236 SNP with the CD4 cell count increase although this SNP is a silent mutation. To our knowledge, this clinical association of *MDR1* 1236 with statistical significance is unprecedented, although its clinical significance remains to be investigated. In conclusion, a large-scale and case-controlled study would be required to test whether SNPs of *MDR1* affect the clinical course during antiretroviral therapy with PIs and the prognosis of infected patients.

Acknowledgements

This work was partly supported by grants for AIDS research from the Ministry of Health, Labor and Welfare of Japan, Grant-in-Aid for Scientific Research (A) from the Japan Society of the Promotion of Science (JSPS) and the Japan Health Sciences Foundation. We thank Dr Yusuke Nakamura (IMSUT) for Japanese SNP information.

References

1. Chaillou S, Durant J, Garraffo R, Georgenthum E, Roptin C, Dunais B, Mondain V, Roger PM & Dellamonica P. Intracellular concentration of protease inhibitors in HIV-1-infected patients: correlation with MDR-1 gene expression and low dose of ritonavir. HIV *Clinical Trials* 2002; 3:493–501.
2. Lee CG, Gottesman MM, Cardarelli CO, Ramachandra M, Jeang KT, Ambudkar SV, Pastan I & Dey S. HIV-1 protease inhibitors are substrates for the *MDR1* multidrug transporter. *Biochemistry* 1998; 37:3594–3601.
3. Hoffmeyer S, Burk O, von Richter O, Arnold HP, Brockmoller J, Johne A, Cascorbi I, Gerloff T, Roots I, Eichelbaum M & Brinkmann U. Functional polymorphisms of the human multidrug-resistance gene: multiple sequence variations and correlation of one allele with P-glycoprotein expression and activity *in vivo*. *Proceedings of the National Academy of Sciences, USA* 2000; 97:3473–3478.
4. Chaudhary PM, Mechetner EB & Roninson IB. Expression and activity of the multidrug resistance P-glycoprotein in human peripheral blood lymphocytes. *Blood* 1992; 80:2735–2739.
5. Drach D, Zhao S, Drach J, Mahadevia R, Gattringer C, Huber H & Andreeff M. Subpopulations of normal peripheral blood and bone marrow cells express a functional multidrug resistant phenotype. *Blood* 1992; 80:2729–2734.

©2004 International Medical Press

6. Sakaeda T, Nakamura T & Okumura K. MDR1 genotype-related pharmacokinetics and pharmacodynamics. *Biological & Pharmaceutical Bulletin* 2002; 25:1391–1400.
7. Yacyshyn B, Maksymowych W & Bowen-Yacyshyn MB. Differences in P-glycoprotein-170 expression and activity between Crohn's disease and ulcerative colitis. *Human Immunology* 1999; 60:677–687.
8. Bellamy WT. P-glycoproteins and multidrug resistance. *Annual Review of Pharmacology & Toxicology* 1996; 36:161–183.
9. Mickley LA, Lee JS, Weng Z, Zhan Z, Alvarez M, Wilson W, Bates SE & Fojo T. Genetic polymorphism in MDR-1: a tool for examining allelic expression in normal cells, unselected and drug-selected cell lines, and human tumors. *Blood* 1998; 91:1749–1756.
10. Saito S, Iida A, Sekine A, Miura Y, Ogawa C, Kawauchi S, Higuchi S & Nakamura Y. Three hundred twenty-six genetic variations in genes encoding nine members of ATP-binding cassette, subfamily B (ABCB/MDR/TAP), in the Japanese population. *Journal of Human Genetics* 2002; 47:38–50.
11. Tanabe M, Ieiri I, Nagata N, Inoue K, Ito S, Kanamori Y, Takahashi M, Kurata Y, Kigawa J, Higuchi S, Terakawa N & Otsubo K. Expression of P-glycoprotein in human placenta: relation to genetic polymorphism of the multidrug resistance (MDR)-1 gene. *Pharmacology & Experimental Therapeutics* 2001; 297:1137–1143.
12. Fellay J, Marzolini C, Meaden ER, Back DJ, Buclin T, Chave JP, Decosterd LA, Furrer H, Opravil M, Pantaleo G, Retelska D, Ruiz L, Schinkel AH, Vernazza P, Eap CB & Telenti A. Response to antiretroviral treatment in HIV-1-infected individuals with allelic variants of the multidrug resistance transporter 1: a pharmacogenetics study. *Lancet* 2002; 359:30–36.
13. Hitzl M, Drescher S, van der Kuip H, Schaffeler E, Fischer J, Schwab M, Eichelbaum M & Fromm MF. The C3435T mutation in the human *MDR1* gene is associated with altered efflux of the P-glycoprotein substrate rhodamine 123 from CD56+ natural killer cells. *Pharmacogenetics* 2001; 11:293–298.
14. Nasi M, Borghi V, Pinti M, Bellodi C, Lugli E, Maffei S, Troiano L, Richeldi L, Mussini C, Esposito R & Cossarizza A. *MDR1* C3435T genetic polymorphism does not influence the response to antiretroviral therapy in drug-naive HIV-positive patients. *AIDS* 2003; 17:1696–1698.
15. Kobayashi N, Nakamura HT, Goto M, Nakamura T, Nakamura K, Sugiura W, Iwamoto A & Kitamura Y. Polymorphisms and haplotypes of the CD209L gene and their association with the clinical courses of HIV-positive Japanese patients. *Japanese Journal of Infectious Diseases* 2002; 55:131–133.
16. Miller G & Lipman M. Release of infectious Epstein-Barr virus by transformed marmoset leukocytes. *Proceedings of the National Academy of Sciences, USA* 1973; 70:190–194.
17. Taipalensuu J, Tornblom H, Lindberg G, Einarsson C, Sjoqvist F, Melhus H, Garberg P, Sjostrom B, Lundgren B & Artursson P. Correlation of gene expression of ten drug efflux proteins of the ATP-binding cassette transporter family in normal human jejunum and in human intestinal epithelial Caco-2 cell monolayers. *Pharmacology & Experimental Therapeutics* 2001; 299:164–170.
18. Yamada H, Kotaki H, Nakamura T & Iwamoto A. Simultaneous determination of the HIV protease inhibitors indinavir, amprenavir, saquinavir, ritonavir and nelfinavir in human plasma by high-performance liquid chromatography. *Journal of Chromatography. B, Biomedical Sciences & Applications* 2001; 755:85–89.
19. Hennessy M, Clarke S, Spiers JP, Kelleher D, Mulcahy F, Hoggard P, Back D & Barry M. Intracellular accumulation of nelfinavir and its relationship to P-glycoprotein expression and function in HIV-infected patients. *Antiviral Therapy* 2004; 9:115–122.
20. Ford J, Cornforth D, Hoggard PG, Cuthbertson Z, Meaden ER, Williams I, Johnson M, Daniels E, Hsyu P, Back DJ & Khoo SH. Intracellular and plasma pharmacokinetics of nelfinavir and M8 in HIV-infected patients: relationship with P-glycoprotein expression. *Antiviral Therapy* 2004; 9:77–84.
21. Schon A, del Mar Ingaramo M & Freire E. The binding of HIV-1 protease inhibitors to human serum proteins. *Biophysical Chemistry* 2003; 105:221–230.
22. Kim RB, Leake BF, Choo EF, Dresser GK, Kubba SV, Schwarz UI, Taylor A, Xie HG, McKinsey J, Zhou S, Lan LB, Schuetz JD, Schuetz EG & Wilkinson GR. Identification of functionally variant MDR1 alleles among European Americans and African Americans. *Clinical Pharmacology & Therapeutics* 2001; 70:189–199.

Received 26 March 2004, accepted 11 August 2004

Bone Marrow Transplantation (2005) 36, 261–262
© 2005 Nature Publishing Group All rights reserved 0268-3369/05 $30.00
www.nature.com/bmt

Correspondence

Unrelated cord blood transplantation for a human immunodeficiency virus-1-seropositive patient with acute lymphoblastic leukemia

Bone Marrow Transplantation (2005) **36,** 261–262. doi:10.1038/sj.bmt.1705028; published online 23 May 2005

The concurrent use of highly active antiretroviral therapy (HAART) improves results of high-dose chemotherapy with autologous stem cell transplantation (SCT) for human immunodeficiency virus-1 (HIV)-associated lymphomas.[1] Recently, successful allogeneic SCT from HLA-matched sibling donors was reported in HIV-infected patients.[2–4] Here, we describe the first case of an HIV-infected patient with acute lymphoblastic leukemia (ALL) who underwent umbilical cord blood transplantation (CBT).

In July 1996, a 23-year-old Japanese woman presented with fever and genital herpes. She was confirmed as seropositive for HIV, probably transmitted from her boyfriend. In March 2001, a real-time quantitative polymerase chain reaction (PCR) analysis showed that the HIV-RNA level was elevated to 25 000 copies/ml (lower limit of detection, 50). The CD4 count decreased to 28/μl. Therefore, HAART consisting of 60 mg stavudine, 300 mg lamivudine, and 600 mg efavirenz was initiated. In July 2001, the HIV-RNA level decreased to 220 copies/ml, and the CD4 count increased to 129/μl. In May 2003, her complete blood count tests showed a white blood cell count (WBC) of 3990/μl with 29% lymphoblasts. Bone marrow (BM) examination showed hypercellularity with 96% lymphoblasts, which were positive for CD4, CD10, CD13, CD19, CD33, CD34, and HLA-DR. Cytogenetic analysis disclosed the presence of t(9;22)(q34;q11) in 12 of 20 metaphases. The $p190^{BCR\text{-}ABL}$ transcript was shown by a reverse transcriptase (RT)-PCR analysis. She was diagnosed as Philadelphia chromosome-positive ALL. She achieved hematological complete remission after two courses of chemotherapy. She has been taking HAART during and after the chemotherapy and her HIV-RNA level continued to be below detectable levels. She was negative for hepatitis B virus surface antigen and anti-hepatitis C virus antibody, and positive for anti-cytomegalovirus antibody. As she had no HLA-matched related or unrelated BM donors, the patient underwent CBT from an unrelated donor with mismatches at two loci (HLA-B and DR) in September 2003 (Figure 1). The numbers of total nucleated cells and CD34-positive cells in the cord

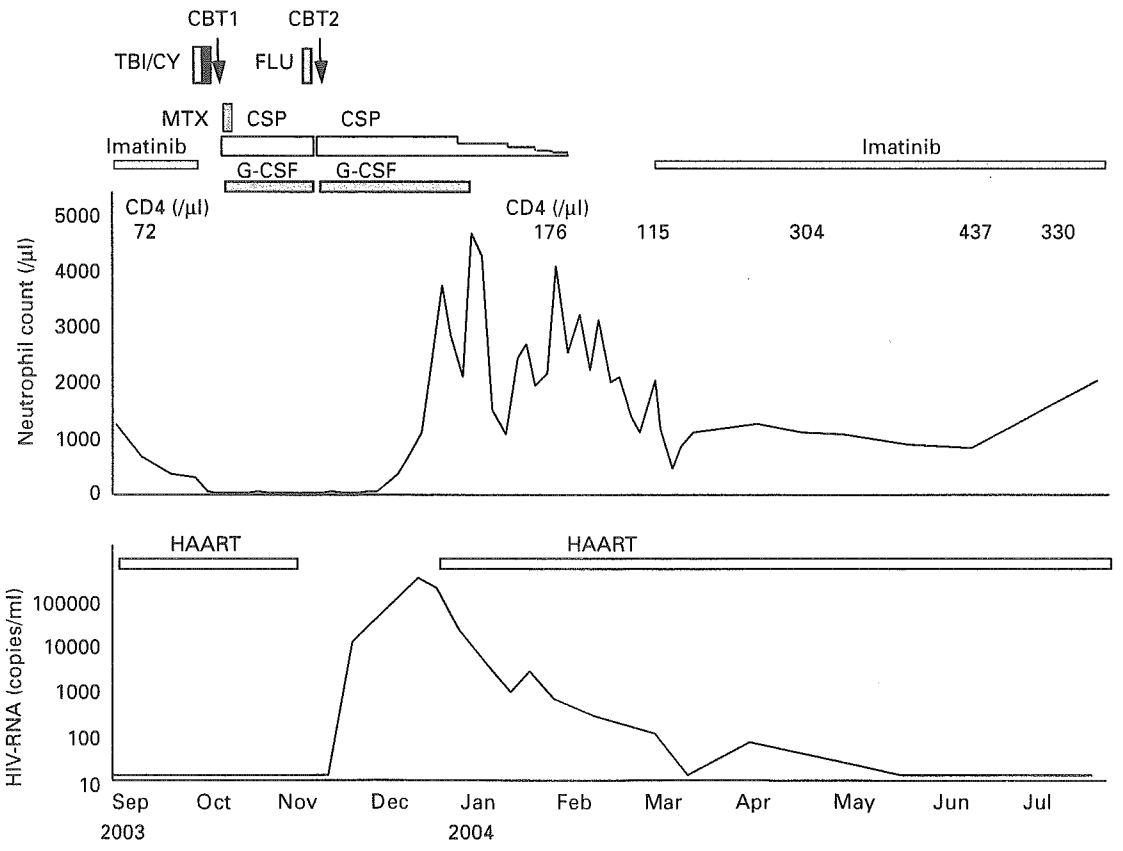

Figure 1 Clinical course of the patient.

blood (CB) unit were 2.9×10^7/kg and 0.76×10^5/kg, respectively. The conditioning regimen included 12 Gy total body irradiation and 120 mg/kg cyclophosphamide. Graft-versus-host disease (GVHD) prophylaxis consisted of cyclosporine and methotrexate. The patient tolerated the procedure well with minimal regimen-related toxicity. Owing to possible myelosuppression, HAART was discontinued on day +28. On day +33, her WBC remained below 100/μl and all of the BM cells were shown to be derived from the recipient. At 40 days after the first CBT, second CBT was performed from an unrelated donor with a one-locus mismatch at HLA-DR. The numbers of total nucleated cells and CD34-positive cells in the CB unit were 2.1×10^7/kg and 0.46×10^5/kg, respectively. The conditioning regimen included 40 mg/m^2 fludarabine for 3 days. Cyclosporine was administered for GVHD prophylaxis. A neutrophil count consistently greater than 500/μl was achieved on day +27. Full donor chimerism of BM cells was shown on day +28. The HIV-RNA level increased to 3×10^6 copies/ml on day +31. After the administration of HAART from day +38, the HIV-RNA levels returned to below detectable levels from day +195, and the CD4 count increased to above 300/μl from day +170. No bacterial or fungal infections were documented during the first and second CBT processes and cytomegalovirus reactivation was successfully treated with ganciclovir and foscarnet. Grade I acute GVHD occurred, but resolved without any additional immunosuppressants. No chronic GVHD was observed. An RT-PCR analysis showed continuous negative test results for the p190$^{BCR\text{-}ABL}$ transcript until the last follow-up evaluation at 15 months post-CBT.

CBT for adults has been associated with a high rate of early transplantation-related mortality (TRM).[5,6] However, our single-institution experience showed a 1-year TRM of 9% and 2-year disease-free survival of 74% in 68 adults after CBT.[7] Both CB donors and the patient in the present study were Japanese. The lesser genetic diversity in a single ethnic population in our studies might be associated with the favorable outcomes of CBT, such as the lower rates of severe acute GVHD. Although our results suggest that CBT is feasible for HIV-infected patients on HAART, the safety and efficacy should be further examined by prospective studies.

A Tomonari[1]
S Takahashi[1]
Y Shimohakamada[1]
J Ooi[1]
K Takasugi[1]
N Ohno[1]
T Konuma[1]
K Uchimaru[1]
A Tojo[1]
T Odawara[2]
T Nakamura[2]
A Iwamoto[2]
S Asano[1]

[1]*Department of Hematology/Oncology, The Institute of Medical Science, The University of Tokyo, Tokyo, Japan; and*
[2]*Department of Infectious Diseases and Applied Immunology, The Institute of Medical Science, The University of Tokyo, Tokyo, Japan*

References

1 Krishnan A, Zaia J, Forman SJ. Should HIV-positive patients with lymphoma be offered stem cell transplants? *Bone Marrow Transplant* 2003; **32**: 741–748.
2 Schlegel P, Beatty P, Halvorsen R, McCune J. Successful allogeneic bone marrow transplant in an HIV-1-positive man with chronic myelogenous leukemia. *J Acquir Immune Defic Syndr* 2000; **24**: 289–290.
3 Sora F, Antinori A, Piccirillo N *et al.* Highly active antiretroviral therapy and allogeneic CD34(+) peripheral blood progenitor cells transplantation in an HIV/HCV coinfected patient with acute myeloid leukemia. *Exp Hematol* 2002; **30**: 279–284.
4 Kang EM, de Witte M, Malech H *et al.* Nonmyeloablative conditioning followed by transplantation of genetically modified HLA-matched peripheral blood progenitor cells for hematologic malignancies in patients with acquired immunodeficiency syndrome. *Blood* 2002; **99**: 698–701.
5 Laughlin MJ, Eapen M, Rubinstein P *et al.* Outcomes after transplantation of cord blood or bone marrow from unrelated donors in adults with leukemia. *N Engl J Med* 2004; **351**: 2265–2275.
6 Rocha V, Labopin M, Sanz G *et al.* Transplants of umbilical-cord blood or bone marrow from unrelated donors in adults with acute leukemia. *N Engl J Med* 2004; **351**: 2276–2285.
7 Takahashi S, Iseki T, Ooi J *et al.* Single institute comparative analysis of unrelated bone marrow transplantation and cord blood transplantation for adult patients with hematological malignancies. *Blood* 2004; **104**: 3813–3820.

Journal of Infection (2006) ■, ■–■

ELSEVIER

BRITISH INFECTION SOCIETY

www.elsevierhealth.com/journals/jinf

CASE REPORT

AIDS-related cerebral toxoplasmosis with hyperintense foci on T1-weighted MR images: A case report

T. Maeda [a,c,*], T. Fujii [b,c], T. Matsumura [b,c], T. Endo [c], T. Odawara [c], D. Itoh [d], Y. Inoue [d], T. Okubo [d], A. Iwamoto [a,b,c], T. Nakamura [c]

[a] *International Research Center for Infectious Diseases, The Institute of Medical Science, The University of Tokyo, 4-6-1 Shirokanedai, Minato-ku, Tokyo 108-8639, Japan*
[b] *Division of Infectious Diseases, Advanced Clinical Research Center, The Institute of Medical Science, The University of Tokyo, 4-6-1 Shirokanedai, Minato-ku, Tokyo 108-8639, Japan*
[c] *Department of Infectious Diseases and Applied Immunology, Research Hospital, The Institute of Medical Science, The University of Tokyo, 4-6-1 Shirokanedai, Minato-ku, Tokyo 108-8639, Japan*
[d] *Department of Radiology, Research Hospital, The Institute of Medical Science, The University of Tokyo, 4-6-1 Shirokanedai, Minato-ku, Tokyo 108-8639, Japan*

Accepted 8 December 2005

KEYWORDS
Toxoplasmosis;
MRI;
AIDS

Summary The neuroradiological findings are helpful for the diagnosis of toxoplasmic encephalitis. The T1 hypersignal intensity foci on brain magnetic resonance (MR) images without contrast enhancement are presented and can be a pathognomonic sign of this disease.
© 2005 The British Infection Society. Published by Elsevier Ltd. All rights reserved.

Introduction

Most toxoplasmic encephalitis is opportunistic infection complicated with the acquired immunodeficiency syndrome (AIDS) and immunosuppressive conditions. The diagnosis of this disease is difficult because of the incompetence of the serological examination for the immunocompromised patients.[1] Although the direct detection method for the pathogen by polymerase chain reaction (PCR) using the cerebrospinal fluid (CSF) has high specificity, the sensitivity of this method is insufficient for definitive diagnosis.[2] We, therefore, have to synthetically diagnose with clinical symptoms, signs, laboratory data, neuroradiological images and the response to anti-toxoplasmosis therapy.

We report here our experience of a unique MR imaging finding of toxoplasmic encephalitis in an

* Corresponding author. International Research Center for Infectious Diseases, The Institute of Medical Science, The University of Tokyo, 4-6-1 Shirokanedai, Minato-ku, Tokyo 108-8639, Japan. Tel: +81 3 5449 5338; fax: +81 3 5449 5427.
E-mail address: tmaeda@ims.u-tokyo.ac.jp (T. Maeda).

0163-4453/$30 © 2005 The British Infection Society. Published by Elsevier Ltd. All rights reserved.
doi:10.1016/j.jinf.2005.12.006

AIDS patient and emphasize the hyperintense foci on T1-weighted MR images that can be one of the pathognomonic MR images of this disease.

Case report

A 44-year-old man with disturbance of consciousness and respiratory insufficiency was admitted to our hospital in April 2005. His consciousness had been rapidly deteriorated and he developed coma 2–3 days before hospitalization. Serological tests of HIV antibodies and *Toxoplasma gondii* IgG antibody were positive, but the *T. gondii* IgM antibody was not detected. The concentration of HIV RNA in plasma was 120,000 copies/ml and the CD 4 cell count was 8 mm^{-3}. The chest X-ray showed bilateral ground glass shadow and *Pneumocystis jiroveci* (carinii) was detected from bronchoalveolar lavage (BAL) fluid. CSF showed mild elevated protein level of 65 mg/dl and pleocytosis, and the opening pressure was over 300 mmH_2O. No malignant cells or microorganisms were detected. *T. gondii* B1-gene fragment was detected by PCR using CSF, therefore, the diagnosis of an AIDS case with toxoplasmic encephalitis was made.[3]

MRI of the brain showed multiple high intensity lesions on T2-weighted image (Fig. 1a) and the corresponding T1-wighted image showed low intensity lesions. Contrast enhanced T1-weighted images showed multiple nodular and ring enhancement lesions.

The chemotherapy with trimethoprim/sulfamethoxazole (TMP/SMX) was very effective and the patient's consciousness level was improved gradually. *P. jiroveci* pneumonia was also cured. MR imaging after 4 weeks of treatment demonstrated that the multiple nodular lesions on T1 and T2-weighted images had significantly been reduced. After 8 weeks of treatment, the contrast enhanced T1-weighted images showed only residual small lesions without contrast enhancement. Interestingly, the hypersignal intensity foci appeared at bilateral basal ganglia obviously after 2 weeks of treatment on the non-enhanced T1-weighted images (Fig. 1b). Corresponding computed tomography (CT) image did not show hemorrhagic or calcified densities (Fig. 1c). These T1 hypersignal intensity foci regressed gradually along with anti-toxoplasmic chemotherapy in proportion to other mass lesions. The T2* (star)-weighted image, which can detect the hemosiderin deposition as hypointensity lesion, operated after 12 weeks of treatment showed no hypointensity at corresponding T1 hypersignal intensity foci on basal ganglia (Fig. 1d).[4] We concluded that the toxoplasmic encephalitis showed the hypersignal intensity foci on T1-weighted MR imaging without hemorrhage or calcification.

Discussion

Toxoplasmic encephalitis progresses rapidly and is life threatening to immunocompromised patients. Therefore, we often have to start the anti-toxoplasmosis therapy when this encephalitis is suspected on the neuroradiologic images and laboratory data. Typically, the toxoplasmic encephalitis lesions on MRI studies appear as T2 hypersignal intensity foci and T1 hypo-isosignal intensity foci, and reveal a rim of enhancement surrounding the edema on contrast enhanced T1-weighted images. Nevertheless, even characteristic foci on these MR imagings are not pathognomonic. Since the differential diagnosis of toxoplasmic encephalitis from other infections or CNS lymphoma is difficult, improvement in the diagnostic methods is an urgent necessity.

In our case, the toxoplasmic encephalitis was diagnosed with the highly specific PCR and confirmed by the response to anti-toxoplasmosis therapy. Brain MRI revealed unusual findings, T1 hypersignal intensity foci, accompanied by typical multiple high intense lesions on T2-weighted image during the treatment. These unique MR findings have been reported on only a few cases of non-HIV/AIDS-related toxoplasmic encephalitis. Terada et al.[5] reported a case of toxoplasmic encephalitis after stem cell transplantation with T1 hypersignal intensity foci. Autopsy revealed the disseminated toxoplasmosis, and coagulative necrosis without hemorrhage or calcification was revealed at corresponding T1 hypersignal intensity foci by neuropathological study. In another post-bone marrow transplantation case, inflammatory and vascular changes without hemorrhage appeared to be the cause of iso or hypersignal intensity rings by the stereotactic biopsy of T1 hypersignal intensity foci.[6] On the other hand, Navia et al.[7] demonstrated that the T1 hypersignal intensity foci were cased by coagulative necrosis with lipid-laden macrophages. The pathophysiological and neuroradiological mechanisms to create these MRI findings are far from clear yet. The reason why the T1 hypersignal intensity foci tend to localize in the basal ganglia is not clear either.[5,6]

CNS lymphoma, which is important for the distinction from toxoplasmic encephalitis, shows T1 hypo-isosignal intensity foci and never shows T1 hypersignal intensity foci except subacute

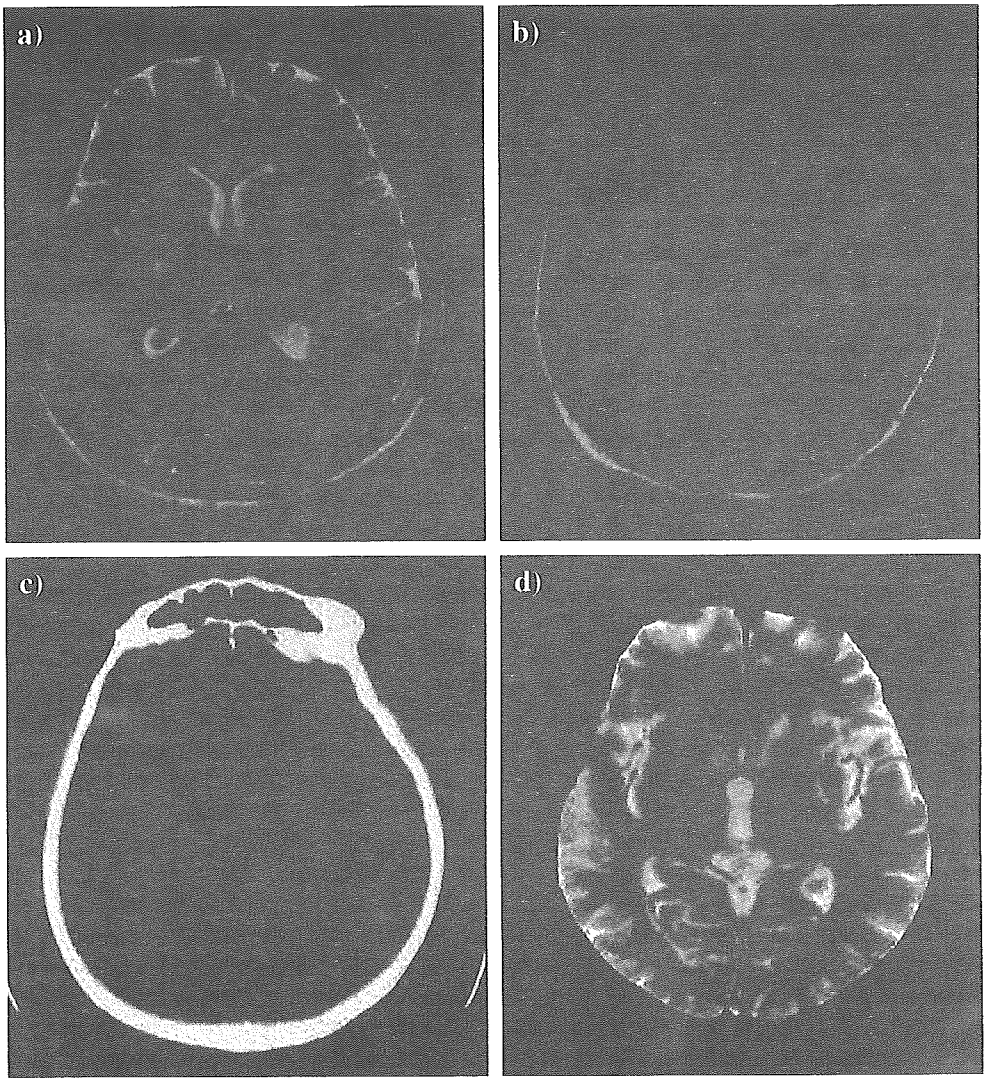

Figure 1 (a) The T2-weighted magnetic resonance image presented multiple high intense lesions. (b) Non-enhanced T1-weighted image showed hypersignal intensity foci at bilateral basal ganglia. (c) The corresponding CT image showed non-hemorrhagic or non-calcified density. (d) The T2* (star)-weighted image showed non-hemorrhagic observations at basal ganglia.

hemorrhage with hypervascular CNS lymphoma.[8,9] However, the CT imaging and T2* (star)-weighted MR imaging can simply distinguish it from the toxoplasmic T1 hypersignal intensity foci without hemorrhage or calcification.

We reported here the unique MRI findings, T1 hypersignal intensity foci, without hemorrhage or calcification on HIV/AIDS-related toxoplasmic encephalitis. It will be helpful for the diagnosis of toxoplasmic encephalitis and may be a pathognomonic finding. Unfortunately, we have not experienced another case of toxoplasmic encephalitis after this case, but we would like to continue to explore this unique MRI finding of this disease.

Acknowledgement

This work was partly supported by the Special Coordination Funds for Promoting Science and Technology of MEXT: strategic cooperation to control emerging and reemerging infections and grants for AIDS research from the Ministry of Health, Labor and Welfare of Japan.

References

1. Luft BJ, Brooks RG, Conley FK, McCabe RE, Remington JS. Toxoplasmic encephalitis in patients with acquired immune deficiency syndrome. *JAMA* 1984;**252**:913–7.

ARTICLE IN PRESS

2. Cingolani A, De Luca A, Ammassari A, Murri R, Linzalone A, Grillo R, et al. PCR detection of *Toxoplasma gondii* DNA in CSF for the differential diagnosis of AIDS-related focal brain lesions. *J Med Microbiol* 1996;**45**:472–6.
3. Castro KG, Ward JW, Slutsker L, Buehler JW, Jaffe HW, Ruth L, et al. 1993 revised classification system for HIV infection and expanded surveillance case definition for aids among adolescents and adults. *Morb Mortal Wkly Rep* 1992; **41**:1–19.
4. Bulte JW, Kraitchman DL. Iron oxide MR contrast agents for molecular and cellular imaging. *NMR Biomed* 2004;**17**: 484–99.
5. Terada H, Kamata N, Yokoyama Y, Ohashi K, Akiyama H, Sakamaki H. T1-hypersignal foci in cerebral toxoplasmosis. *Riv Neuroradiol* 2001;**14**:665–7 [Case report].
6. Dietrich U, Maschke M, Dorfler A, Prumbaum M, Forsting M. MRI of intracranial toxoplasmosis after bone marrow transplantation. *Neuroradiology* 2000;**42**:14–8.
7. Navia BA, Petito CK, Gold JW, Cho ES, Jordan BD, Price RW. Cerebral toxoplasmosis complicating the acquired immune deficiency syndrome: clinical and neuropathological findings in 27 patients. *Ann Neurol* 1986;**19**:224–38.
8. Jenkins CN, Colquhoun IR. Characterization of primary intracranial lymphoma by computed tomography: an analysis of 36 cases and a review of the literature with particular reference to calcification haemorrhage and cyst formation. *Clin Radiol* 1998;**53**:428–34 [Review].
9. Rubenstein J, Fischbein N, Aldape K, Burton E, Shuman M. Hemorrhage and VEGF expression in a case of primary CNS lymphoma. *J Neurooncol* 2002;**58**:53–6.

研究成果の刊行に関する一覧表

雑誌

発表者氏名	論文タイトル名	発表誌名	巻号	ページ	出版年
Tokoro M, Asai T, Kobayashi S, Takeuchi T, Nozaki T	Identification and characterization of two isoenzymes of methionine γ-lyase from Entamoeba histolytica	J Biol Chem	278	42717 ~42727	2003
Haghighi A, Kobayashi S, Takeuchi T, Thammapelerd N, Nozaki T	Geographic diversity among genotypes of Entamoeba histolytica field isolates	J Clin Microbiol	41	3678 ~3756	2003
Tachibana H, Takekoshi M, Cheng X-J, Nakata Y, Takeuchi T, Ihara S	Bacterial expression of a human monoclonal antibody-alkaline phosphatase conjugate specific for Entamoeba histolytica	Clin Diagn Lab Immunol	11	216 ~218	2003
Tachibana H, Watanabe K, Cheng X-J, Tsukamoto H, Kaneda Y, Takeuchi T, Ihara S, Petri WA Jr	VH3 gene usage in neutralizing human antibodies specific for Entamoeba histolytica Gal/GalNAc lecetin heavy subunit	Infect Immun	71	4313 ~4319	2003
Makioka A, Kumagai M, Kobayashi S, Takeuchi T	Entamoeba invadens: inhibition of excystation and metacystic development by aphidicolin	Exp Parasitol	103	61 ~67	2003
Kumagai M, Makioka A, Takeuchi T, Nozaki T	Molecular cloning and characterization of a protein farnesyl transferase from the enteric protozoan parasite Entamoeba histolytica	J Biol Chem	279	2316 ~2323	2003
Makioka A, Kumagai M, Kobayashi S, Takeuchi T	Involvement of protein kinase C and phosphatidylinositol 3-kinase in the excystation and metacystic development of Entamoeba invadens	Parasitol Res	91	204 ~208	2003
Tachibana H, Cheng X-J, Masuda G, Horiki N, Takeuchi T	Evaluation of recombinant fragments of Entamoeba histolytica Gal/GalNAc letin intermediate subunit for the serodiagnosis of amebiasis	J Clin Microbiol	42	1069 ~1074	2004

発表者氏名	論文タイトル名	発表誌名	巻号	ページ	出版年
Iwashita J, Sato Y, Kobayashi S, Takeuchi T, Abe T	Isolation and functional analysis of chk2 homologue from Entamoeba histolytica	Parasitol Int	54	21~27	2005
Cheng X-J, Yoshihara E, Takeuchi T, Tachibana H	Molecular characterization of peroxiredoxin from Entamoeba moshkovskii and a comparison with Entamoeba histolytica	Mol Biochem Parasitol	138	195 ~203	2004
Makioka A, Kumagai M, Kobayashi S, Takeuchi T	Entamoeba invadens: cysteine protease inhibitors block excystation and metacystic development	Exp Parasitol	109	27~32	2005
Khalifa SAM, Imai E, Kobayashi S, Haghighi A, Hayakawa E, Takeuchi T	Growth-promoting effect of iron-sulfur proteins on axenic cultures of Entamoeba dispar	Parasite	in press		2006
Kobayashi S, Imai E, Haghighi A, Khalifa SAM, Tachibana H, Takeuchi T	Axenic cultivation of Entamoeba dispar in newly designed yeast extract-iron -gluconic acid-dihydroxy-acetone-serum medium	J Parasitol	91	1~4	2005
小林正規、前田卓哉、竹内　勤	赤痢アメーバの抗原検出法、シンポジウム「寄生虫症診断に用いる検査キットの諸問題	Clin Parasitol	in press		2006
Makioka A, Kumagai M, Takeuchi T, Nozaki T	Characterization of protein geranylgeranyl transferase I from the enteric protist Entamoeba histolytica	Mol Biochem Parasitol	in press		2006
Makioka A, Kumagai M, Kobayashi S, Takeuchi T	Effect of artificial gastrointestinal fluid on excystation and metacystic development of Entamoeba invadens	Parasitol Res	in press		2006

THE JOURNAL OF BIOLOGICAL CHEMISTRY
Vol. 278, No. 43, Issue of October 24, pp. 42717–42727, 2003
Printed in U.S.A.
© 2003 by The American Society for Biochemistry and Molecular Biology, Inc.

Identification and Characterization of Two Isoenzymes of Methionine γ-Lyase from *Entamoeba histolytica*

A KEY ENZYME OF SULFUR-AMINO ACID DEGRADATION IN AN ANAEROBIC PARASITIC PROTIST THAT LACKS FORWARD AND REVERSE TRANS-SULFURATION PATHWAYS*

Received for publication, December 5, 2002, and in revised form, August 11, 2003
Published, JBC Papers in Press, August 14, 2003, DOI 10.1074/jbc.M212414200

Masaharu Tokoro‡, Takashi Asai‡, Seiki Kobayashi‡, Tsutomu Takeuchi‡, and Tomoyoshi Nozaki§¶‖

From the ‡Department of Tropical Medicine and Parasitology, Keio University School of Medicine, Tokyo 160-8582, Japan, the §Department of Parasitology, National Institute of Infectious Diseases, Tokyo 162-8640, Japan, and the ¶Precursory Research for Embryonic Science and Technology, Japan Science and Technology Corporation, Tokyo 190-0012, Japan

To better understand the metabolism of sulfur-containing amino acids, which likely plays a key role in a variety of cell functions, in *Entamoeba histolytica*, we searched the genome data base for genes encoding putative orthologs of enzymes known to be involved in the metabolism. The search revealed that *E. histolytica* possesses only incomplete cysteine-methionine conversion pathways in both directions. Instead, this parasite possesses genes encoding two isoenzymes of methionine γ-lyase (EC 4.4.1.11, EhMGL1/2), which has been implicated in the degradation of sulfur-containing amino acids. The two amebic MGL isoenzymes, showing 69% identity to each other, encode 389- and 392-amino acid polypeptides with predicted molecular masses of 42.3 and 42.7 kDa and pIs of 6.01 and 6.63, respectively. Amino acid comparison and phylogenetic analysis suggested that these amebic MGLs are likely to have been horizontally transferred from the Archaea, whereas an MGL from another anaerobic protist *Trichomonas vaginalis* has MGL isotypes that share a common ancestor with bacteria. Enzymological and immunoblot analyses of the partially purified native amebic MGL confirmed that both of the MGL isotypes are expressed in a comparable amount predominantly in the cytosol and form a homotetramer. Recombinant EhMGL1 and 2 proteins catalyzed degradation of L-methionine, DL-homocysteine, L-cysteine, and *O*-acetyl-L-serine to form α-keto acid, ammonia, and hydrogen sulfide or methanethiol, whereas activity toward cystathionine was negligible. These two isoenzymes showed notable differences in substrate specificity and pH optimum. In addition, we showed that EhMGL is an ideal target for the development of new chemotherapeutic agents against amebiasis by demonstrating an amebicidal effect of the methionine analog trifluoromethionine on trophozoites in culture (IC_{50} 18 μM) and that this effect of trifluoromethionine was completely abolished by the addition of the MGL-specific inhibitor DL-propargylglycine.

Entamoeba histolytica is a causative agent of amebiasis, which annually affects an estimated 48 million people and results in 70,000 deaths (1). The most common clinical presentation of amebiasis is amebic dysentery and colitis; extraintestinal abscesses, *i.e.* hepatic, pulmonary, and cerebral, however, are also common and often lethal. This microaerophilic anaerobe has been considered to be a unique eukaryotic organism because it apparently lacks organelles typical of eukaryotic organisms such as mitochondria, the rough endoplasmic reticulum, and the Golgi apparatus (2). However, a recent demonstration of genes encoding mitochondrial proteins, *i.e.* cpn60 and pyridine nucleotide transhydrogenase (3), together with electron micrographic demonstration of the rough endoplasmic reticulum and the Golgi apparatus (4), suggested the presence of a residual organelle of mitochondria (called crypton or mitosome) (5, 54) and also indicated that this group of parasitic protists possess a unique organelle organization. This parasite also reveals numerous unusual aspects in its metabolism (6), highlighted by the lack of the tricarboxylic acid cycle (7) and glutathione metabolism (8). In addition, recent studies suggesting the horizontal transfer of genes encoding a variety of fermentation enzymes from bacteria (9), and genes encoding malic enzyme and acetyl-CoA synthase from the Archaea (10) have placed this protozoan organism at a unique position in eukaryotic evolution.

One of these unique metabolic pathways found in this parasite is the biosynthetic and degradative pathway of sulfur-containing amino acids, especially cysteine, which has been demonstrated to be essential for the growth and various cellular activities of amoebae (11, 12). Sulfur-containing amino acid metabolism varies among organisms (Fig. 1, also reviewed in Ref. 13). In mammals, cysteine is produced solely from incorporated methionine and serine via *S*-adenosylmethionine, homocysteine, and cystathionine in a pathway called the reverse trans-sulfuration pathway. In contrast, plants, fungi, and some bacteria have a so-called sulfur assimilation pathway to fix inorganic sulfur onto a serine derivative (*O*-acetylserine,

* This work was supported by a grant for Precursory Research for Embryonic Science and Technology (PRESTO), Japan Science and Technology Corporation, Grants-in-aid for Scientific Research on Priority Areas from the Ministry of Education, Culture, Sports, Science and Technology of Japan (15019120, 15590378), a grant for Research on Emerging and Re-emerging Infectious Diseases from Ministry of Health, Labor, and Welfare of Japan, and a grant from the Project to Promote Development of Anti-AIDS Pharmaceuticals from Japan Health Sciences Foundation (SA 14706) (to T. N.). The costs of publication of this article were defrayed in part by the payment of page charges. This article must therefore be hereby marked "*advertisement*" in accordance with 18 U.S.C. Section 1734 solely to indicate this fact.

The nucleotide sequence(s) reported in this paper has been submitted to the DDBJ/GenBank™/EBI Data Bank with accession number(s) AB094499 and AB094500.

‖ To whom correspondence should be addressed: 1-23-1 Toyama, Shinjuku-ku, Tokyo, 162-8640, Japan. Tel.: 81-3-5285-1111 (ext. 2733); Fax: 81-3-5285-1173; E-mail: nozaki@nih.go.jp.

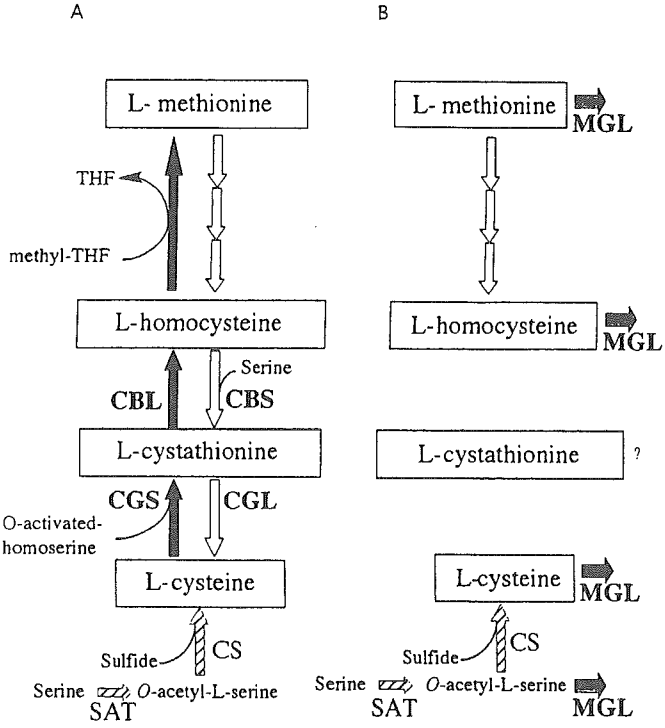

FIG. 1. **A schematic representation of sulfur-containing amino acid metabolism in general (*A*) and in *Entamoeba* (*B*).** Only enzymes that belong to the γ-subfamily of PLP-dependent enzymes are shown (in *bold*), together with CS and CBS, which belong to the β-family, and SAT. Biochemical steps involved in both forward and reverse trans-sulfuration reactions are indicated by *filled* and *open arrows*, respectively. Genes encoding the first three steps of the reverse trans-sulfuration pathway have been identified in the *E. histolytica* genome data base (data not shown). *Gray arrows* indicate reactions catalyzed by MGLs and *hatched arrows* indicate sulfur assimilatory steps we previously reported (14, 15).

OAS)[1] to synthesize cysteine. These organisms are also capable of converting cysteine into methionine via a trans-sulfuration sequence in the opposite orientation (also called the methionine biosynthetic pathway). We previously demonstrated that *E. histolytica* possesses the sulfur assimilatory cysteine biosynthetic pathway, and is capable of producing cysteine *de novo* (14, 15). We have also demonstrated (15) that major enzymes in this pathway, serine acetyltransferase (SAT) and cysteine synthase (CS), play a central role in the control of the intracellular cysteine concentrations, and in the antioxidative stress defense mechanism of this gluthathione-lacking parasite (8).

One important question remaining about the sulfur-containing amino acid metabolism in this parasite, and also in anaerobic protists in general, is how these parasites degrade toxic sulfur-containing amino acids since they possess apparently incomplete trans-sulfuration pathways in both the forward and reverse orientation (data not shown, see the present study). Thus, in order to better understand the metabolism, particularly degradation, of these sulfur-containing amino acids in *E. histolytica*, we attempted to isolate other essential genes encoding proteins involved in sulfur amino acid metabolism.

We identified and characterized two isotypes of the unique enzyme, methionine γ-lyase (MGL; EC 4.4.1.11) and their encoding genes, which, we propose, function in the degradation of sulfur amino acids in this parasite. We show a line of evidence suggesting that the MGL genes and their proteins were likely derived from the Archaea by horizontal transfer as shown for other metabolic enzymes in this parasite (10). In addition, we also demonstrate that the methionine analog trifluoromethionine (TFMET) has a cytotoxic effect on amebic trophozoites that is abolished by a specific inhibitor of MGL, indicating that MGL is exploitable as an attractive target for the development of new amebicidal compounds.

EXPERIMENTAL PROCEDURES

Chemicals and Reagents—L-methionine, L-cysteine, DL-homocysteine, OAS, *O*-succinyl-L-homocysteine, *O*-acetyl-L-homoserine, DL-propargylglycine (PPG), 3-methyl-2-benzothiazolinone hydrazon hydrochloride, trichloroacetic acid, pyridoxal 5′-phosphate (PLP), and other chemicals were commercial products of the highest purity available unless otherwise stated. TFMET was a gift from Dr. Cyrus J. Bacchi (Haskins Laboratories and Department of Biology, Pace University, New York).

Microorganisms and Cultivation—Trophozoites of *E. histolytica* strain HM-1:IMSS cl-6 (16) were maintained axenically in Diamond's BI-S-33 medium (11) at 35.5 °C. Trophozoites were harvested at the late-logarithmic growth phase 2–3 days after inoculation of one-twelfth to one-sixth of a total culture volume. After the cultures were chilled on ice for 5 min, trophozoites were collected by centrifugation at 500 × *g* for 10 min at 4 °C and washed twice with ice-cold phosphate-buffered saline, pH 7.4. Cell pellets were stored at −80 °C until use.

Search of the Genome Data Base of E. histolytica—The *E. histolytica* genome data base at the Institute for Genomic Research (TIGR, //www.tigr.org/tdb/) was searched using the TBLASTN algorithm with protein sequences corresponding to the PLP-attachment site of cysteine- and methionine-metabolizing enzymes (PROSITE access number PS00868). This motif is conserved among the γ−subfamily (α-family) of PLP enzymes (for the classification of PLP enzymes used in this study, see Ref. 17), *i.e.* cystathionine γ-lyase (CGL), cystathionine γ-synthase (CGS), and cystathionine β-lyase (CBL) from a variety of organisms. We also searched for amebic orthologs that belong to the β-family of PLP enzymes using the PLP-attachment site from CS of *E. histolytica* and cystathionine β-synthase (CBS) from yeast and mammals.

Cloning of E. histolytica MGL1 and MGL2 and Production of their Recombinant Proteins—Based on nucleotide sequences of the protein-encoding region of the two putative amebic MGL genes (*EhMGL1* and *EhMGL2*), two sets of primers, shown below, were designed to amplify the open reading frames (ORF) of *EhMGL1* and to construct plasmids to produce glutathione *S*-transferase (GST)-EhMGL fusion proteins. The two sense and two antisense primers contained the *Sma*I restriction site (underlined) either prior to the translation initiation site or next to the stop codon (*bold*), respectively. The primers used are: *EhMGL1* (sense), 5′-CAT<u>CCCGGG</u>**GATG**ACTGCTCAAGATATTACTACTAC-T-3′ (37-mer); *EhMGL1* (antisense), 5′-TAG<u>CCCGGG</u>**ATTA**CCAAAG-CTCTAATGCTTGTTTTAA-3′ (37-mer); *EhMGL2* (sense), 5′-CAT<u>CCC-GGG</u>**TATG**TCTCAATTGAAGGATTTACAAACA-3′ (37-mer); *EhMGL2* (antisense), 5′-TAG<u>CCCGGG</u>**ATTA**GCATTGTTCAAGAGCTTGTTTT-AA-3′ (37-mer).

The cDNA library of *E. histolytica* trophozoites constructed in a lambda phage (14) was used as the template for polymerase chain reaction (PCR) using the following parameters. An initial step for denaturation and *rTaq* (Takara Bio Inc., Shiga, Japan) activation at 94 °C for 15 min was followed by 35 cycles of denaturation at 94 °C for 30 s, annealing at 45 °C for 30 s, and extension at 72 °C for 1 min. A final step at 72 °C for 10 min was used to complete the extension. Approximately 1.1-kb PCR fragments were obtained and cloned into the *Sma*I site of a pGEX-6P-1 expression vector (Amersham Biosciences K.K., Tokyo, Japan). The final constructs were designated as pGEX6P1/MGL1 and pGEX6P1/MGL2, respectively.

Nucleotide sequences were confirmed by using appropriate synthetic sequencing primers, a BigDye Terminator Cycle Sequencing Ready Reaction Kit, and an ABI PRISM 310 genetic analyzer (Applied Biosystems Japan Ltd., Tokyo, Japan), according to the manufacturer's protocol. To express the recombinant proteins in *Escherichia coli*, pGEX6P1/MGL1 and pGEX6P1/MGL2 were introduced into *BL21 (DE3)* (Novagen Inc., Madison, WI) host cells. Expression of the GST-MGL1 and GST-MGL2 fusion proteins was induced with 1 mM isopro-

[1] The abbreviations used are: OAS, *O*-acetylserine; TFMET, trifluoromethionine; TIGR, The Institute for Genomic Research; SAT, serine acetyltransferase; CS, cysteine synthase; MGL, methionine γ-lyase; PPG, DL-propargylglycine; PLP, pyridoxal 5′-phosphate; CGL, cystathionine γ-lyase; CGS, cystathionine γ-synthase; CBL, cystathionine β-lyase; CBS, cystathionine β-synthase; ORF, open reading frame; GST, glutathione *S*-transferase; rEhMGL, recombinant EhMGL; NJ, Neighbor-Joining; MP, maximum parsimony; ML, maximum likelihood; MOPS, 4-morpholinepropanesulfonic acid; MES, 4-morpholineethanesulfonic acid.